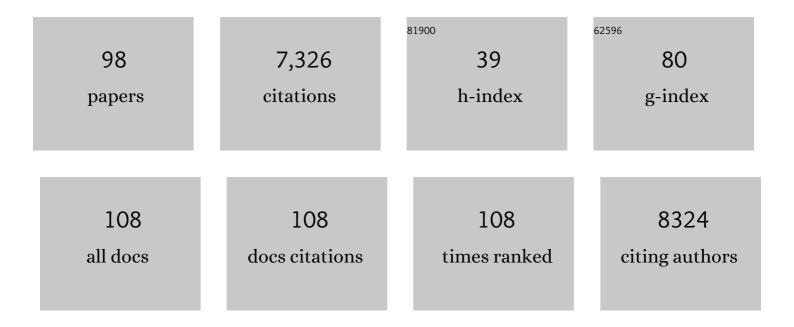
List of Publications by Year in descending order

Source: https://exaly.com/author-pdf/3742729/publications.pdf Version: 2024-02-01



KAMII HUUDAC

#	Article	IF	CITATIONS
1	Neurodegenerative and functional signatures of the cerebellar cortex in m.3243A > G patients. Brain Communications, 2022, 4, fcac024.	3.3	2
2	Layer-dependent functional connectivity methods. Progress in Neurobiology, 2021, 207, 101835.	5.7	67
3	Effects of MP2RAGE B1+ sensitivity on inter-site T1 reproducibility and hippocampal morphometry at 7T. NeuroImage, 2021, 224, 117373.	4.2	17
4	Quantitative and simultaneous measurement of oxygen consumption rates in rat brain and skeletal muscle using ¹⁷ 0 MRS imaging at 16.4T. Magnetic Resonance in Medicine, 2021, 85, 2232-2246.	3.0	7
5	Determining laminar neuronal activity from BOLD fMRI using a generative model. Progress in Neurobiology, 2021, 207, 102055.	5.7	10
6	Sub-millimetre resolution laminar fMRI using Arterial Spin Labelling in humans at 7 T. PLoS ONE, 2021, 16, e0250504.	2.5	27
7	Improvement of sensitivity and specificity for laminar BOLD fMRI with double spin-echo EPI in humans at 7 T. NeuroImage, 2021, 241, 118435.	4.2	11
8	Perfusion MRI using endogenous deoxyhemoglobin as a contrast agent: Preliminary data. Magnetic Resonance in Medicine, 2021, 86, 3012-3021.	3.0	17
9	A dynamical model of the laminar BOLD response. NeuroImage, 2020, 204, 116209.	4.2	78
10	Direct visualization and characterization of the human zona incerta and surrounding structures. Human Brain Mapping, 2020, 41, 4500-4517.	3.6	21
11	Unraveling the contributions to the neuromelanin-MRI contrast. Brain Structure and Function, 2020, 225, 2757-2774.	2.3	41
12	Feedback contribution to surface motion perception in the human early visual cortex. ELife, 2020, 9, .	6.0	7
13	Dynamic behavior of the locus coeruleus during arousal-related memory processing in a multi-modal 7T fMRI paradigm. ELife, 2020, 9, .	6.0	43
14	European Ultrahighâ€Field Imaging Network for Neurodegenerative Diseases (EUFIND). Alzheimer's and Dementia: Diagnosis, Assessment and Disease Monitoring, 2019, 11, 538-549.	2.4	17
15	Locus coeruleus imaging as a biomarker for noradrenergic dysfunction in neurodegenerative diseases. Brain, 2019, 142, 2558-2571.	7.6	219
16	Aerobic Exercise Training Improves Cerebral Blood Flow and Executive Function: A Randomized, Controlled Cross-Over Trial in Sedentary Older Men. Frontiers in Aging Neuroscience, 2019, 11, 333.	3.4	86
17	Non-BOLD contrast for laminar fMRI in humans: CBF, CBV, and CMRO2. NeuroImage, 2019, 197, 742-760.	4.2	96
18	Distortion-matched T1 maps and unbiased T1-weighted images as anatomical reference for high-resolution fMRI. NeuroImage, 2018, 176, 41-55.	4.2	32

#	Article	IF	CITATIONS
19	Cortical depth profiles of luminance contrast responses in human V1 and V2 using 7 T fMRI. Human Brain Mapping, 2018, 39, 2812-2827.	3.6	59
20	The impact of correction on <scp>MP2RAGE</scp> cortical <scp>T</scp> ₁ and apparent cortical thickness at 7 <scp>T</scp> . Human Brain Mapping, 2018, 39, 2412-2425.	3.6	38
21	Neuroimaging with ultra-high field MRI: Present and future. Neurolmage, 2018, 168, 1-6.	4.2	33
22	Anatomic & metabolic brain markers of the m.3243A>G mutation: A multi-parametric 7T MRI study. NeuroImage: Clinical, 2018, 18, 231-244.	2.7	15
23	Techniques for blood volume fMRI with VASO: From low-resolution mapping towards sub-millimeter layer-dependent applications. NeuroImage, 2018, 164, 131-143.	4.2	101
24	Individualized parcellation of the subthalamic nucleus in patients with Parkinson's disease with 7T MRI. NeuroImage, 2018, 168, 403-411.	4.2	106
25	Impact of acquisition and analysis strategies on cortical depth-dependent fMRI. NeuroImage, 2018, 168, 332-344.	4.2	71
26	Linking brain vascular physiology to hemodynamic response in ultra-high field MRI. NeuroImage, 2018, 168, 279-295.	4.2	137
27	The impact of ultra-high field MRI on cognitive and computational neuroimaging. NeuroImage, 2018, 168, 366-382.	4.2	93
28	High-resolution in vivo imaging of human locus coeruleus by magnetization transfer MRI at 3T and 7T. NeuroImage, 2018, 168, 427-436.	4.2	104
29	Resolving laminar activation in human V1 using ultra-high spatial resolution fMRI at 7T. Scientific Reports, 2018, 8, 17063.	3.3	53
30	Examples of sub-millimeter, 7T, T1-weighted EPI datasets acquired with the T123DEPI sequence. Data in Brief, 2018, 20, 415-418.	1.0	4
31	Ultra-high resolution blood volume fMRI and BOLD fMRI in humans at 9.4â€ [−] T: Capabilities and challenges. NeuroImage, 2018, 178, 769-779.	4.2	44
32	Optimization of simultaneous multislice EPI for concurrent functional perfusion and BOLD signal measurements at 7T. Magnetic Resonance in Medicine, 2017, 78, C1-C1.	3.0	0
33	Comparison of 3 T and 7 T ASL techniques for concurrent functional perfusion and BOLD studies. NeuroImage, 2017, 156, 363-376.	4.2	34
34	On the importance of modeling fMRI transients when estimating effective connectivity: A dynamic causal modeling study using ASL data. NeuroImage, 2017, 155, 217-233.	4.2	24
35	Echo-time dependence of the BOLD response transients – A window into brain functional physiology. NeuroImage, 2017, 159, 355-370.	4.2	23
36	Tonotopic maps in human auditory cortex using arterial spin labeling. Human Brain Mapping, 2017, 38, 1140-1154.	3.6	16

KAMIL ULUDAG

#	Article	IF	CITATIONS
37	Optimization of simultaneous multislice EPI for concurrent functional perfusion and BOLD signal measurements at 7T. Magnetic Resonance in Medicine, 2017, 78, 121-129.	3.0	24
38	Pulsatility of Lenticulostriate Arteries Assessed by 7 Tesla Flow MRI—Measurement, Reproducibility, and Applicability to Aging Effect. Frontiers in Physiology, 2017, 8, 961.	2.8	39
39	Determining Excitatory and Inhibitory Neuronal Activity from Multimodal fMRI Data Using a Generative Hemodynamic Model. Frontiers in Neuroscience, 2017, 11, 616.	2.8	98
40	Subthalamic Nucleus Deep Brain Stimulation: Basic Concepts and Novel Perspectives. ENeuro, 2017, 4, ENEURO.0140-17.2017.	1.9	106
41	Ultra-High Field MRI Post Mortem Structural Connectivity of the Human Subthalamic Nucleus, Substantia Nigra, and Globus Pallidus. Frontiers in Neuroanatomy, 2016, 10, 66.	1.7	42
42	Reproducibility and Reliability of Quantitative and Weighted T1 and T2â^— Mapping for Myelin-Based Cortical Parcellation at 7 Tesla. Frontiers in Neuroanatomy, 2016, 10, 112.	1.7	49
43	fMRI Adaptation between Action Observation and Action Execution Reveals Cortical Areas with Mirror Neuron Properties in Human BA 44/45. Frontiers in Human Neuroscience, 2016, 10, 78.	2.0	18
44	170 relaxation times in the rat brain at 16.4 tesla. Magnetic Resonance in Medicine, 2016, 75, 1886-1893.	3.0	6
45	Functional cerebral blood volume mapping with simultaneous multi-slice acquisition. NeuroImage, 2016, 125, 1159-1168.	4.2	22
46	Volumetric imaging with homogenised excitation and static field at 9.4 T. Magnetic Resonance Materials in Physics, Biology, and Medicine, 2016, 29, 333-345.	2.0	23
47	The effect of spatial resolution on decoding accuracy in fMRI multivariate pattern analysis. NeuroImage, 2016, 132, 32-42.	4.2	101
48	Affected functional networks associated with sentence production in classic galactosemia. Brain Research, 2015, 1616, 166-176.	2.2	14
49	Functional MRI Dynamics. , 2015, , 81-87.		Ο
50	fMRI: From Nuclear Spins to Brain Functions. Biological Magnetic Resonance, 2015, , .	0.4	9
51	Physiologically informed dynamic causal modeling of fMRI data. NeuroImage, 2015, 122, 355-372.	4.2	109
52	Combining fMRI with Other Modalities: Multimodal Neuroimaging. Biological Magnetic Resonance, 2015, , 739-768.	0.4	2
53	Physiology and Physics of the fMRI Signal. Biological Magnetic Resonance, 2015, , 163-213.	0.4	5
54	Ultra-high field magnetic resonance imaging of the basal ganglia and related structures. Frontiers in Human Neuroscience, 2014, 8, 876.	2.0	47

#	Article	IF	CITATIONS
55	General overview on the merits of multimodal neuroimaging data fusion. NeuroImage, 2014, 102, 3-10.	4.2	179
56	Regional effects of magnetization dispersion on quantitative perfusion imaging for pulsed and continuous arterial spin labeling. Magnetic Resonance in Medicine, 2013, 69, 524-530.	3.0	9
57	Spatial representations of temporal and spectral sound cues in human auditory cortex. Cortex, 2013, 49, 2822-2833.	2.4	50
58	On the feasibility of concurrent human TMS-EEG-fMRI measurements. Journal of Neurophysiology, 2013, 109, 1214-1227.	1.8	34
59	Retinotopic maps and hemodynamic delays in the human visual cortex measured using arterial spin labeling. NeuroImage, 2012, 59, 4044-4054.	4.2	20
60	Network-based statistics for a community driven transparent publication process. Frontiers in Computational Neuroscience, 2012, 6, 11.	2.1	6
61	Convergence of human brain mapping tools: Neuronavigated TMS Parameters and fMRI activity in the hand motor area. Human Brain Mapping, 2012, 33, 1107-1123.	3.6	56
62	Differential effects of intranasal insulin and caffeine on cerebral blood flow. Human Brain Mapping, 2012, 33, 280-287.	3.6	26
63	Quantifying the Link between Anatomical Connectivity, Gray Matter Volume and Regional Cerebral Blood Flow: An Integrative MRI Study. PLoS ONE, 2011, 6, e14801.	2.5	42
64	On the numerically predicted spatial BOLD fMRI specificity for spin echo sequences. Magnetic Resonance Imaging, 2011, 29, 1195-1204.	1.8	20
65	Functional localization in the human brain: Gradientâ€echo, spinâ€echo, and arterial spin″abeling fMRI compared with neuronavigated TMS. Human Brain Mapping, 2011, 32, 341-357.	3.6	74
66	Relationship of the BOLD Signal with VEP for Ultrashort Duration Visual Stimuli (0.1 to 5 ms) in Humans. Journal of Cerebral Blood Flow and Metabolism, 2010, 30, 449-458.	4.3	23
67	Predictors of Response to Treadmill Exercise in Stroke Survivors. Neurorehabilitation and Neural Repair, 2010, 24, 567-574.	2.9	57
68	To dip or not to dip: Reconciling optical imaging and fMRI data. Proceedings of the National Academy of Sciences of the United States of America, 2010, 107, E23; author reply E24.	7.1	32
69	Interleaved TMS/CASL: Comparison of different rTMS protocols. NeuroImage, 2010, 49, 612-620.	4.2	37
70	Neural activity-induced modulation of BOLD poststimulus undershoot independent of the positive signal. Magnetic Resonance Imaging, 2009, 27, 1030-1038.	1.8	37
71	Comparison of pulsed arterial spin labeling encoding schemes and absolute perfusion quantification. Magnetic Resonance Imaging, 2009, 27, 1039-1045.	1.8	72
72	Latin American Brain Mapping Network (LABMAN). NeuroImage, 2009, 47, 312-313.	4.2	7

#	Article	IF	CITATIONS
73	An integrative model for neuronal activity-induced signal changes for gradient and spin echo functional imaging. NeuroImage, 2009, 48, 150-165.	4.2	381
74	Transient and sustained BOLD responses to sustained visual stimulation. Magnetic Resonance Imaging, 2008, 26, 863-869.	1.8	46
75	Dynamics and nonlinearities of the BOLD response at very short stimulus durations. Magnetic Resonance Imaging, 2008, 26, 853-862.	1.8	54
76	Decreases in ADC observed in tissue areas during activation in the cat visual cortex at 9.4 T using high diffusion sensitization. Magnetic Resonance Imaging, 2008, 26, 889-896.	1.8	29
77	Direct measurement of oxygen extraction with fMRI using 6% CO2 inhalation. Magnetic Resonance Imaging, 2008, 26, 961-967.	1.8	45
78	Simultaneous PET-MRI: a new approach for functional and morphological imaging. Nature Medicine, 2008, 14, 459-465.	30.7	1,008
79	The Influence of Moderate Hypercapnia on Neural Activity in the Anesthetized Nonhuman Primate. Cerebral Cortex, 2008, 18, 2666-2673.	2.9	144
80	Magnetic Field Distribution and Signal Decay in Functional MRI in Very High Fields (up to 9.4 T) Using Monte Carlo Diffusion Modeling. International Journal of Biomedical Imaging, 2007, 2007, 1-7.	3.9	5
81	Investigating the post-stimulus undershoot of the BOLD signal—a simultaneous fMRI and fNIRS study. NeuroImage, 2006, 30, 349-358.	4.2	115
82	Relevance of depth resolution for cerebral blood flow monitoring by near-infrared spectroscopic bolus tracking during cardiopulmonary bypass. Journal of Thoracic and Cardiovascular Surgery, 2006, 132, 1172-1178.	0.8	34
83	Frontiers of brain mapping using MRI. Journal of Magnetic Resonance Imaging, 2006, 23, 945-957.	3.4	58
84	Letter to the editor. Magnetic Resonance in Medicine, 2004, 51, 1088-1089.	3.0	12
85	Cytochrome-c-oxidase redox changes during visual stimulation measured by near-infrared spectroscopy cannot be explained by a mere cross talk artefact. NeuroImage, 2004, 22, 109-119.	4.2	39
86	Towards a standard analysis for functional near-infrared imaging. NeuroImage, 2004, 21, 283-290.	4.2	213
87	Separability and cross talk: optimizing dual wavelength combinations for near-infrared spectroscopy of the adult head. Neurolmage, 2004, 22, 583-589.	4.2	101
88	Coupling of cerebral blood flow and oxygen consumption during physiological activation and deactivation measured with fMRI. NeuroImage, 2004, 23, 148-155.	4.2	230
89	Modeling the hemodynamic response to brain activation. NeuroImage, 2004, 23, S220-S233.	4.2	1,023
90	Caffeine alters the temporal dynamics of the visual BOLD response. NeuroImage, 2004, 23, 1402-1413.	4.2	113

#	Article	IF	CITATIONS
91	Investigating the physiology of brain activation with MRI. , 2004, , .		Ο
92	Neurovascular coupling analyzed non-invasively in the human brain. NeuroReport, 2004, 15, 63-66.	1.2	43
93	Functional brain imaging by CW-NIRS coregistered by blood flow monitors. , 2003, , .		Ο
94	Noninvasive monitoring of cerebral blood flow by a dye bolus method: Separation of brain from skin and skull signals. Journal of Biomedical Optics, 2002, 7, 464.	2.6	88
95	Cross talk in the Lambert-Beer calculation for near-infrared wavelengths estimated by Monte Carlo simulations. Journal of Biomedical Optics, 2002, 7, 51.	2.6	119
96	Habituation of the Visually Evoked Potential and Its Vascular Response: Implications for Neurovascular Coupling in the Healthy Adult. NeuroImage, 2002, 17, 1-18.	4.2	126
97	Dopplersonographic measurement of global cerebral circulation time using echo contrast-enhanced ultrasound in normal individuals and patients with arteriovenous malformations. Ultrasound in Medicine and Biology, 2002, 28, 453-458.	1.5	35
98	<title>Noninvasive cerebral blood flow monitoring by a dye bolus method:separation of extra- and intracerebral absorption changes by frequency-domain spectroscopy</title> . , 2001, , .		2